# Seismic Amplification by Deep Subsurface and Proposal of a New Proxy

Nagao, Takashi

(Citation)
Engineering, Technology & Applied Science Research,10(1):5157-5163

(Issue Date)
2020-02

(Resource Type)
journal article

(Version)
Version of Record



(URL)
https://hdl.handle.net/20.500.14094/90006824

# Seismic Amplification by Deep Subsurface and Proposal of a New Proxy

Takashi Nagao
Research Center for Urban Security and Safety
Kobe University
Kobe, Japan
nagao@people.kobe-u.ac.jp

***Abstract*—Codes of practice and ground motion prediction equations involve ground structure proxies to account for seismic amplification. Although the ground consists of both shallow and deep subsurface, proxies are mainly related to the shallow subsurface as it is shallow subsurface information that is mostly available. However, as deep subsurface seismic amplification is not negligible, it may not be appropriate to use shallow subsurface proxies. In this study, the relationship between shallow and deep subsurface seismic amplification factors is discussed on the basis of S-wave velocity profile data from Japanese KiK-net strong-motion observation system stations. The correlation between typical proxies such as the average S-wave velocity of the top 30m of the ground surface and the seismic amplification factor was examined. Although there was a negative correlation between the two, the degree of the correlation was weak. A new proxy showing stronger correlations with the seismic amplification factor is proposed and its effectiveness is demonstrated.**

***Keywords-seismic amplification; Vs30; S-wave velocity; deep subsurface***

## I. INTRODUCTION

Earthquake ground motions are amplified as they propagate through the ground, thus differences in ground characteristics are considered in design earthquake ground motions and ground motion prediction equations (GMPEs). The concept of using surface soil conditions to select design earthquake ground motions and GMPEs has been pervasive for years since [1]. A typical ground structure proxy to account for seismic amplification is the average S-wave velocity from the surface down to 30m beneath the surface (*Vs*30). *Vs*30 can be easily calculated from ground data without seismic response analysis and a correlation between *Vs*30 and seismic amplification has been noted [2, 3]. For this reason, although discussions on the appropriateness of using *Vs*30 as a proxy continue [4, 5], *Vs*30 is widely used at present and has been introduced as a proxy in National Earthquake Hazards Reduction program (NEHRP) [6], AASHTO [7], Eurocode8 [8], and various other models [9, 10] and GMPEs [11, 12]. Note that the ground's natural period is used as a proxy in Japanese codes of practice [13, 14].

The ground consists of shallow and deep subsurface layers, and the boundary between the shallow and deep subsurface layers is referred to as engineering bedrock. This is a rigid layer with shear rigidity that does not deteriorate even during strong earthquakes. Both *Vs*30 and the natural period are mainly related to the shallow subsurface. S-wave velocities are approximately 100m/s in soft soil, 300m/s or more in stiff soil, 500m/s or more in rock, and 700m/s or more in engineering bedrock. However, the seismic bedrock beneath the deep subsurface layer can have S-wave velocities of 3000m/s or more. The degree of seismic amplification depends greatly on S-wave velocity changes in the ground, with the shallow subsurface having a velocity change of about a factor of two to four and the deep subsurface change being approximately a factor of five. Therefore, the deep subsurface often has a greater seismic amplification than the shallow subsurface. Some studies have pointed out the importance of deep subsurface to seismic amplification [15], and others have claimed that accurate evaluation of deep subsurface seismic amplification is important for assessing seismic ground motion [16]. However, the S-wave velocity structure from the engineering bedrock to the seismic bedrock varies greatly from site to site, and ground structures down to the seismic bedrock at many sites have not been clarified in detail. For this reason, few studies have systematically discussed deep subsurface seismic amplification, and none have tested the validity of explaining shallow and deep subsurface seismic amplification in proxies related to the shallow subsurface such as *Vs*30. This study discusses the differences in seismic amplification between shallow and deep subsurface layers using information on actual ground structures and determines the optimal proxy for seismic amplification. For simplicity, the shallow and deep subsurface will be described as characteristics of the deep subsurface hereinafter.

## II. METHOD

In this study, KiK-net [17] was targeted, which is a network of strong-motion observation seismographs developed in Japan. Vertical-array strong-motion observation is performed on the ground surface and underground at KiK-net sites, with sensors installed deeper than the engineering bedrock in boreholes in rock or stiff soil. Seismic ground motion amplification factors can be discussed by analyzing the spectral ratios of strong-motion records from the ground surface and in the borehole. However, as most of the observation points do not reach the seismic bedrock in their boreholes, only those amplifications

Corresponding author Takashi Nagao

with deep subsurface degrees of effect that differ from point to point can be discussed. Therefore, in this study we calculate and discuss theoretical amplification factors based on the S-wave velocity structure from the ground surface to the seismic bedrock. S-wave velocity structure from the ground surface to the borehole sensor's installation depth is obtained using P-S logging data at the KiK-net sites. For the S-wave velocity structure from the borehole sensor installation depth to the seismic bedrock, S-wave velocity structure information from the Japan Seismic Hazard Information Station (J-SHIS) [18] is used. Thus, S-wave velocity structure from the ground surface to the seismic bedrock is obtained by combining KiK-net and J-SHIS S-wave velocity structure information. In this study we used 615 data points.

Figure 1 shows the cumulative distributions of shallow and deep subsurface depths, with the red line indicating shallow subsurface and the blue line denoting the deep subsurface. The cumulative probability for sites with a shallow subsurface depth of less than 30m is 62%. Although more than half of the sites include deep subsurface information in $V_S30$, the percentage of that information in the total is not very high**.** KiK-net stations are often installed at sites with thin deposits such as mountainous areas [19], but only two sites have deep subsurface depths of 30m or less, and more than 50% of the sites have deep subsurface depths of 400m or more, with 30% exceeding 1000m. Sites with shallow subsurface thicknesses of 2m or less are generally regarded as rock or stiff soil sites, 94% of the data points are from deep subsurface depths deeper than 100m and 27% points have depths deeper than 1000m. It is obvious that there are limitations in expressing the seismic amplification using shallow subsurface proxies.

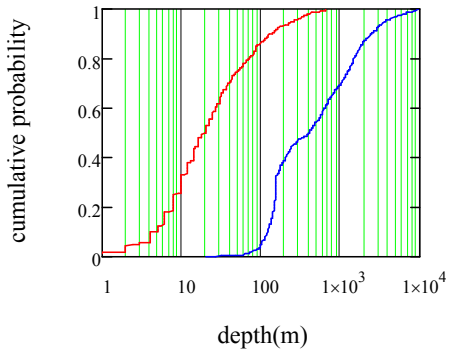


Fig. 1. Cumulative layer thickness distributions of shallow and deep subsurface

$Vs30$ is the time-averaged S-wave velocity of the top 30m of the ground and is expressed as:

$$Vs30 = 30 / \Sigma (h_i/Vs_i) \quad (1)$$

where $h_i$ is the thickness of soil layer $i$ (m), and $Vs_i$ is the S-wave velocity of soil layer $i$ (m/s).

The NEHRP [6] classifies ground types into five groups (class A–E) based on $Vs30$ (Table I). Japanese highway bridge design specifications [13] classify ground types into three groups (types 1 to 3) based on the natural period of shallow subsurface (Table II). The numbers in parentheses in Tables I and II indicate the percentage of data points included in each category. NEHRP class C sites are relatively common in this study. As for correlation with Japanese highway bridge design specifications, type 1 ground, which corresponds to hard ground, is the most common at 80%. The reason for this is that KiK-net stations are mainly installed in areas with relatively thin deposit layers [19]. Shallow and deep subsurface transfer functions were calculated using SH-wave multiple-reflection theory under an assumption of horizontally stratified ground to evaluate the seismic amplification factor. For the quality factor ($Q$) representing inelastic damping, the values shown in Table III were used in accordance with J-SHIS [18]. Regarding obtained transfer functions, we focused on the 0.1–10.0Hz range as that frequency range strongly influences structure and ground stability during earthquakes, and examined maximum amplitude frequencies (peak frequencies) and peak amplitudes.

TABLE I. GROUND TYPE CLASSIFICATIONS IN NEHRP

| Site class | $Vs30$ (m/s) |
|---|---|
| A (1) | $1500 < Vs30$ |
| B (12) | $760 < Vs30 \leq 1500$ |
| C (57) | $360 < Vs30 \leq 760$ |
| D (28) | $180 < Vs30 \leq 360$ |
| E (2) | $Vs30 \leq 180$ |

TABLE II. GROUND TYPE CLASSIFICATION IN JAPAN'S HIGHWAY BRIDGE DESIGN SPECIFICATIONS

| Ground type | Natural period: $Ts$ (s) |
|---|---|
| 1 (80) | $Ts \leq 0.2$ |
| 2 (17) | $0.2 < Ts \leq 0.6$ |
| 3 (3) | $0.6 < Ts$ |

TABLE III. QUALITY FACTOR

| $Vs$ (m/s) | $Q$ |
|---|---|
| $Vs < 600$ | 60 |
| $600 \leq Vs < 1000$ | 100 |
| $1000 \leq Vs < 2000$ | 150 |
| $2000 \leq Vs < 3000$ | 200 |
| $3000 \leq Vs$ | 300 |

## III. EXAMPLES OF S-WAVE VELOCITY PROFILES AND SEISMIC AMPLIFICATION FACTORS

Figure 2 shows the S-wave velocity profiles of the sites under consideration, with AOMH13, IBRH10, and SZOH42 selected as examples of points having low $Vs30$ values, HRSH02, NGSH01, and SIGH03 selected as medium points, and FKIH01, ISKH06, and OITH06 are selected as high $Vs30$ value examples. The numbers in parentheses after the station code are the $Vs30$ values of each site. In the low $Vs30$ group, S-wave velocity reaches 1500m/s at a depth of 224m at station SZOH42. In contrast, the S-wave velocity is only about 400m/s at 200m at AOMH13 and IBRH10. For the medium $Vs30$ group, the S-wave velocity exceeds 2000m/s at 30m and reaches 3000m/s at 150m at HRSH02, whereas at NGSH01, the S-wave velocity reaches 1900m/s at 18m without showing large increase until 1000m. For SIGH03, the S-wave velocity is 530m/s at 30m and does not exceed 2000m/s until 350m. For the high $Vs30$ group, the S-wave velocity exceeds 2000m/s at 20m at FKIH01, whereas at OITH06 the S-wave velocity

reaches 1700m/s at 100m. At ISKH06, the S-wave velocity does not exceed 2000m/s until 260m. In summary, even for the same *Vs*30 values, S-wave velocity structures down to the seismic bedrock vary greatly from point to point.

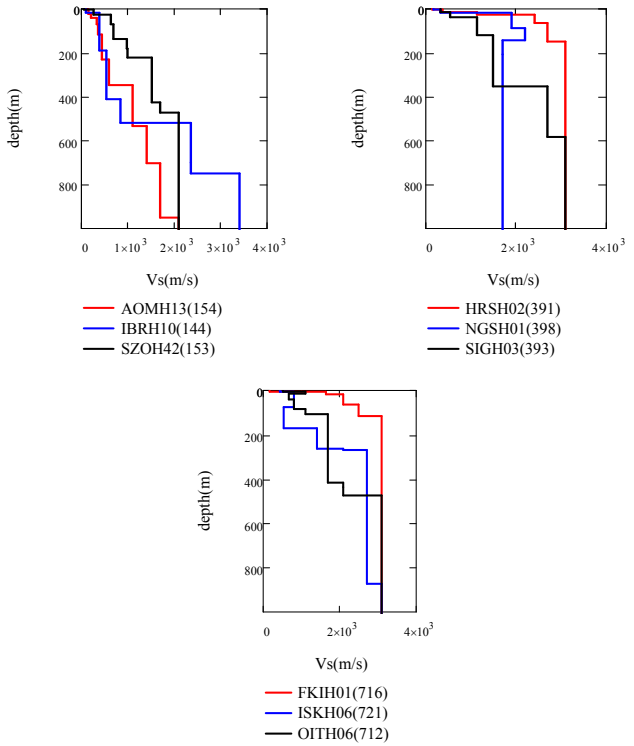


Fig. 2. S-wave velocity profile

Figure 3 shows the transfer functions for the respective points, where the red solid lines denote shallow subsurface transfer functions and the blue solid lines represent deep subsurface transfer functions. For the low *Vs*30 group, the shallow subsurface ($f_s$) and deep subsurface ($f_d$) peak frequencies are generally consistent, but deep subsurface peak amplitudes ($A_d$) are much larger than shallow subsurface values ($A_s$), with amplification factor ratios ranging from 1.7 to 2.6. Furthermore, for the station IBRH10, although the deep subsurface transfer function shows a large amplification of approximately 10 at 0.3Hz and 0.7Hz, there are no clear peaks in the shallow subsurface transfer functions. The $f_s$ and $f_d$ roughly agree with each other at the three points where *Vs*30 is moderate, but $A_d$ is 1.5–2.2 times greater than $A_s$. At the three points where *Vs*30 is large, $f_d$ and $f_s$ agree with each other at IBRH10, but the shallow subsurface amplification factor is almost 1, whereas the deep subsurface transfer function shows a large amplification at several frequencies. Additionally, peaks can be seen at frequencies lower than the three points exemplified as a medium *Vs*30 at 2.2Hz at stations ISKH06 and 0.73Hz at station OITH06. At FKIH01, the $A_d$ is 17.7, which is the second largest $A_d$ after SZOH42 among the nine points shown. Thus, because of differences in deep subsurface S-wave velocity structures, the amplification factors greatly differ even for similar *Vs*30 values.

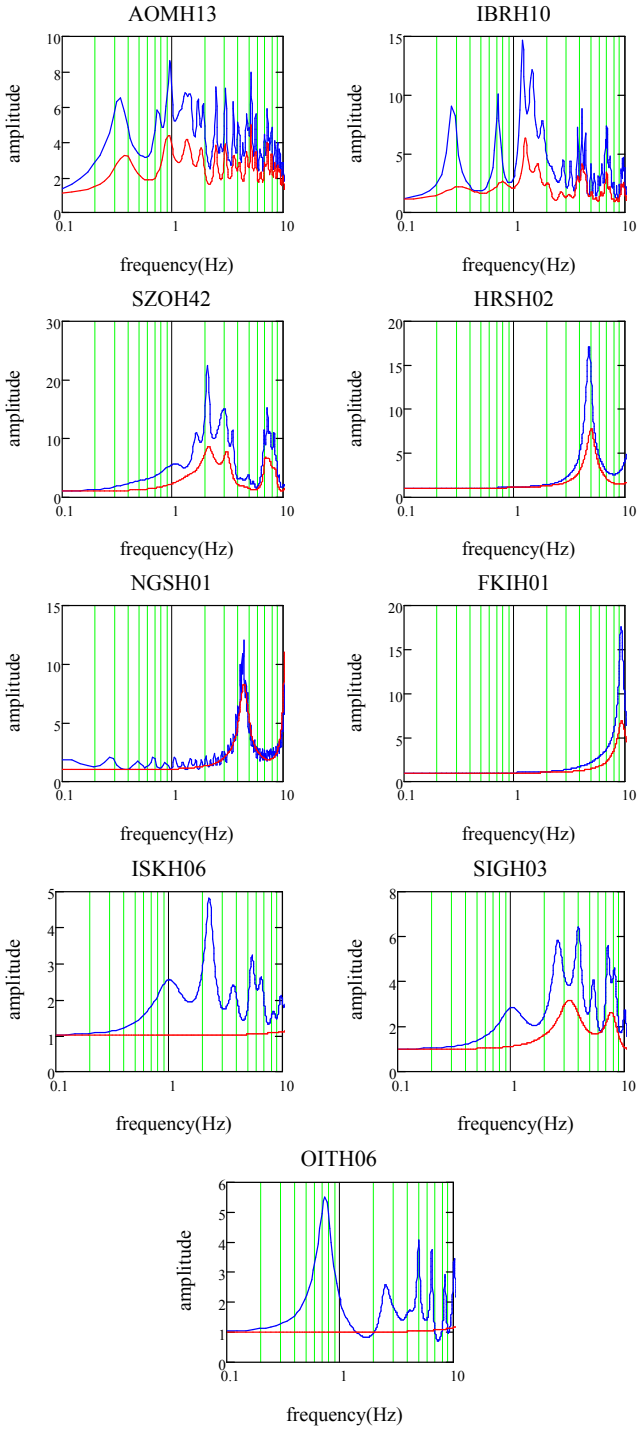


Fig. 3. Transfer function

## IV. RESULTS AND DISCUSSION

### A. Relationship between Shallow and Deep Subsurface Peak Amplification Factors

Figure 4 shows the relationship between $A_s$ and $A_d$ which are plotted on the horizontal and vertical axes respectively. Plotting on a double logarithmic chart shows a positive

correlation between the two peak amplification factors, however, the variation is large. Figure 5 shows the frequency distribution of peak amplification factor ratios. The solid line represents a probability density function assuming a lognormal distribution, and the distribution of the peak amplification factor ratios can be approximated by a lognormal distribution. The mean value was 2.39 and the standard deviation was 0.74. It was thus shown that the assessment of deep subsurface seismic amplification is crucial for properly evaluating earthquake ground motions and GMPEs. The characteristic of the lognormal distribution is that the distribution's right-side tail is heavy and the maximum ratio value is as large as 5.64. The red broken line in Figure 4 represents the regression equation (2) obtained by performing a linear regression analysis on double logarithmic plots with a determination coefficient of 0.76.

$$\log A_d = 0.484 + 0.766 \log A_s \quad (2)$$

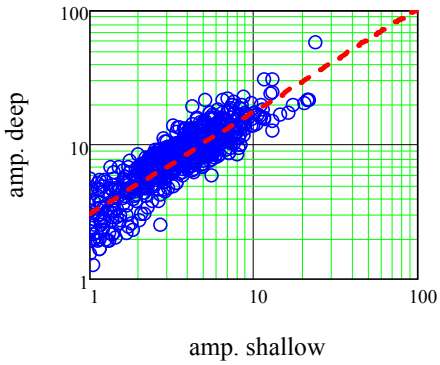


Fig. 4. Relationship between $A_s$ and $A_d$

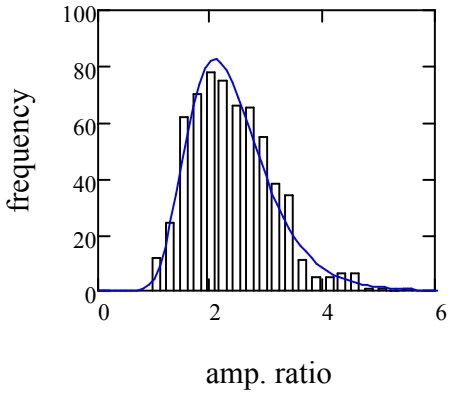


Fig. 5. Frequency distribution of peak amplification ratio

### *B. Relationship between Peak Frequency and Peak Amplification Factor*

Figure 6 shows the relationship between peak frequency and peak amplification factors. Both shallow and deep subsurface show large scatters between frequency and amplification, with no correlation observed. A low peak frequency indicates a thick deposit layer or soft deposit layer at the site, and the amplification factor is assumed to be large. However, this is not the case in practice. At station AOMH13, although $f_s$, $f_d$ are as low as 1Hz, $A_s$ is 5.0 and $A_d$ is 8.6, and the amplification factors are lower than at NGSH01, which have a $f_s$, $f_d$ values of 4.5Hz, $A_s$ 6.9, and $A_d$ of 17.7. The reason for this is the difference in the deposited layer thickness. Although the S-wave velocity is low and the deposited layer is very thick at AOMH13, peak amplification is not large due to damping effects. This means that the peak amplification factor is determined by complex combinations of parameters such as S-wave velocity and layer thickness in each soil layer, and the peak frequency of the ground is not an appropriate proxy for seismic amplification.

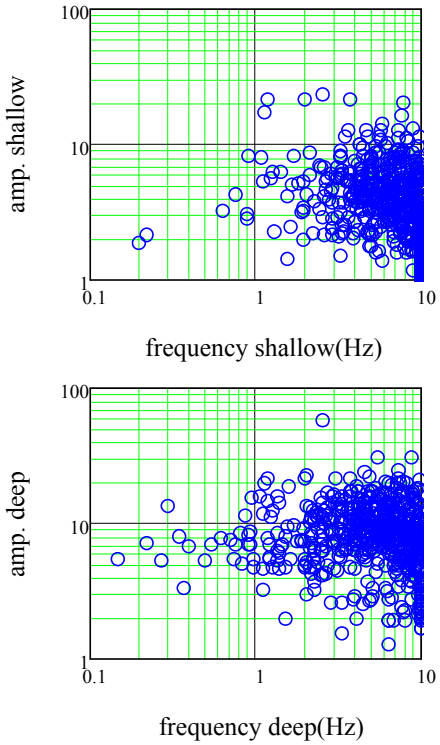


Fig. 6. Relationship between peak frequency and peak amplification factor

### *C. Relationship between Vs30 and Peak Amplification Factor*

Figure 7 shows the relationships between $Vs30$ and $A_s$, $A_d$. For $Vs30$, there is less variation with $A_s$ and $A_d$ than with peak frequency, and there is a weak negative correlation. In particular, the variation is small where $Vs30$ exceeds 1000m/s. Therefore, it can be said that $Vs30$ is appropriate as a seismic amplification proxy for NEHRP class A sites. However, in regions where $Vs30$ is less than 1000m/s, the variation is large, with particularly large variations from 760m/s to 500m/s, but it is reduced in regions where $Vs30$ is 500m/s or less. The reason for this reduction in variation is that $A_d$ has an upper limit value limited to approximately 20, whereas the $A_d$ lower limit value is increased when $Vs30$ decreases. Therefore, the reduced variation where $Vs30$ is 500m/s or less does not necessarily indicate a strong correlation between $Vs30$ and peak amplification. As a result, $A_d$ has the largest variation in NEHRP class C sites, which differs slightly from the $A_s$ case as $A_s$ is 1 in many cases at sites with a large $Vs30$. However, the

variation is also very large from 500m/s to 760m/s. The red broken line in Figure 7 represents the regression equation obtained through linear regression analysis (3), (4).

$$\log A_s = 2.865 - 0.877 \log Vs30 \quad (3)$$

$$\log A_d = 3.173 - 0.858 \log Vs30 \quad (4)$$

The determination coefficients are 0.40 for $A_s$ and 0.49 for $A_d$, which are not high. However, $A_d$ had a slightly higher determination coefficient than $A_s$ despite $Vs30$ being considered an indicator of shallow subsurface geological structures. The reason is that the variation of $A_s$ is greater than that of $A_d$ on the logarithmic scale under the same $Vs30$ condition. Furthermore, because KiK-net stations used in this study are installed in locations with relatively thin deposits [19], approximately 40% of the points had deep subsurface appearing at less than 30m beneath the surface. Therefore, it is considered that the relatively large number of points with deep subsurface information included in $Vs30$ led to high correlations between amplification factors by deep subsurface and $Vs30$. As a method of regression analysis, a constraint condition may be considered such that $A_d$ becomes 1 when $Vs30$ becomes 2000m/s. However, the determination coefficient is lower than the determination coefficient resulting from (3) and (4).

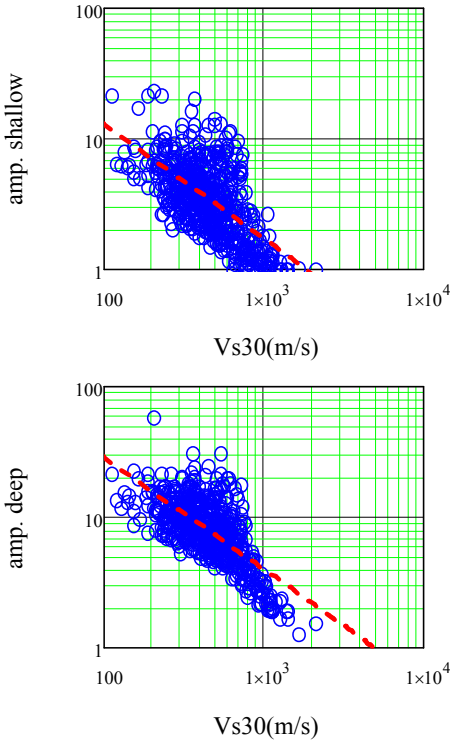


Fig. 7. Relationship between $Vs30$ and peak amplification factor

## V. PROPOSAL OF A NEW PROXY

The reason why $Vs30$ and peak amplification show negative correlations is that $Vs30$ is high at rocky sites with a low amplification factor, and $Vs30$ is low in soft sediment sites with a high amplification factor. The results described above also indicated a negative correlation between the two parameters, but the variation was very large. To solve this problem, we compared the amplification factors of three ground structures with different S-wave velocity contrasts in top 30m and the same $Vs30$ at 300m/s, as shown in Table IV. The deep subsurface transfer function is illustrated in Figure 8. Case 1, which has the highest S-wave velocity contrast, shows the largest $A_d$, and Case 3, which has the lowest contrast, shows the smallest $A_d$. The same results were obtained for $A_s$. $Vs30$ has a certain effectiveness as an index for simply expressing the complicated ground structure to 30m of the surface layer, but information on the impedance contrast is not necessarily sufficiently expressed by only $Vs30$. Therefore, in this study, we propose a modified $Vs30$ that corrects $Vs30$ using the impedance contrasts of the ground surface to 30m as:

$$Vs30_{mod} = \sqrt{\frac{Vs_s}{Vs_{d30}}} \cdot Vs30 \quad (5)$$

where $Vs30_{mod}$ is the modified $Vs30$, $Vs_s$ is the S-wave velocity of the ground surface, and $Vs_{d30}$ is the S-wave velocity 30m beneath the surface.

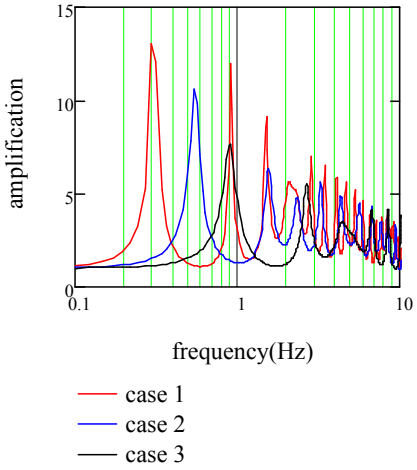


Fig. 8. Transfer function

TABLE IV. MODEL GROUND STRUCTURE

| Case 1 | | Case 2 | | Case 3 | |
|---|---|---|---|---|---|
| ***h* (m)** | ***Vs* (m/s)** | ***h* (m)** | ***Vs* (m/s)** | ***h* (m)** | ***Vs* (m/s)** |
| 5 | 100 | 10 | 200 | 50 | 300 |
| 45 | 500 | 40 | 400 | | |
| 50 | 1000 | 50 | 1000 | 50 | 1000 |
| - | 2500 | - | 2500 | - | 2500 |

*h*: layer thickness

A comparative study of the correlation between the modified $Vs30$ and peak amplification factor yielded an S-wave velocity ratio between the ground surface and 30m of 0.5 power. Figure 9 shows the relationship between the modified $Vs30$, $Vs30$, and $A_d$ for the model ground. The red circle denotes the modified $Vs30$ and the gray triangle indicates the $Vs30$. The use of the modified $Vs30$ clarifies the negative correlation between the average S-wave velocities and peak amplifications. The relationship between the modified $Vs30$ and peak amplification factor is illustrated in Figure 10. The

variation is reduced compared to the relationship of $Vs30$ with both $A_s$ and $A_d$. In particular, because the increasing tendency in the variation for a specific $Vs30$ range is alleviated, the new proxy is applicable for all ground categories. The red broken line in Figure 10 represents the regression equation obtained using a regression analysis ((6)-(7)):

$$\log A_s = 2.734 - 0.948 \log Vs30_{mod} \quad (6)$$

$$\log A_d = 2.853 - 0.844 \log Vs30_{mod} \quad (7)$$

The obtained determination coefficients are 0.63 for $A_d$ and 0.61 for $A_s$, which are significantly larger than the $Vs30$ regression equations. Thus, the modified $Vs30$ is more useful as a seismic amplification proxy than $Vs30$.

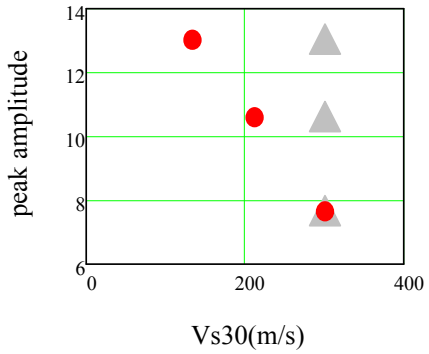


Fig. 9. Relationship between $Vs30$, modified $Vs30$, and $A_d$

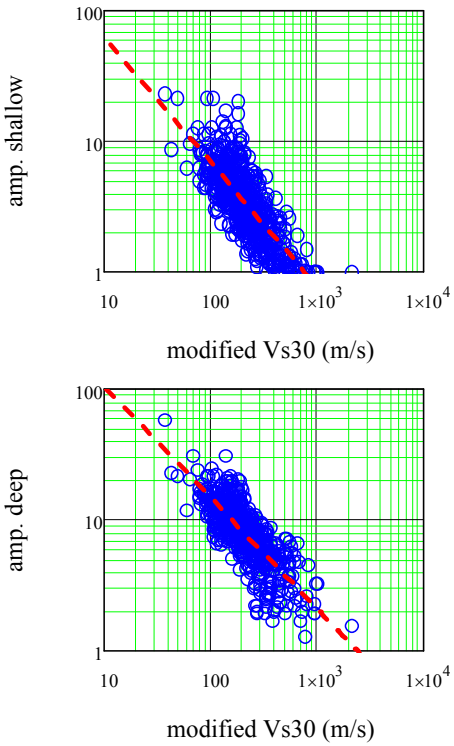


Fig. 1. Relationship between modified $Vs30$ and peak amplification factor

## VI. Conclusion

In this study, the theoretical seismic amplification characteristics of shallow and deep subsurface were examined using P-S logging data from the KiK-net strong-motion observation network and deep ground data from J-SHIS. In this study the following conclusions were obtained:

- The deep subsurface to shallow subsurface seismic amplification ratios have a mean of 2.39 and a standard deviation of 0.74, and seismic amplification considering only the shallow subsurface underestimates the seismic amplification of the whole ground. Assessment of the deep subsurface's amplification characteristics is crucial for properly evaluating earthquake ground motions and GMPEs.
- Examining the correlation between the typical proxies and seismic amplification factors demonstrated that the shallow subsurface peak frequency is not correlated with seismic amplification factors, and $Vs30$ shows a weak negative correlation with seismic amplification factors. However, $Vs30$ varies greatly relative to seismic amplification factors. To reduce this variation, we proposed a modified $Vs30$ that considers the S-wave velocity ratios of the ground surface at the depth of 30m. The variation in the relationship between the modified $Vs30$ and the seismic amplification factor is reduced compared with that using the conventional $Vs30$. Therefore, seismic amplification factors can be evaluated more accurately with the modified $Vs30$ than the conventional $Vs30$.

## Acknowledgments

The author appreciates KiK-net and J-SHIS for providing the ground structure data.

## References

[1] H. B. Seed, C. Ugas, J. Lysmer, "Site-dependent spectra for earthquake-resistant design", Bulletin of the Seismological Society of America. Vol. 66, No. 1, pp. 221-243, 1976

[2] R. D. Borcherdt, "Estimates of site-dependent response spectra for design (methodology and justification)", Earthquake Spectra, Vol. 10, No. 4, pp. 617–653, 1994

[3] R. Dobry, R. D. Borcherdt, C. B. Crouse, I. M. Idriss, W. B. Joyner, G. Martin, M. S. Power, E. E. Rinne, R. B. Seed, "New site coefficients and site classification system used in recent building seismic code provisions", Earthqake Spectra, Vol. 16, No. 1, pp. 41–67, 2000

[4] S. Castellaro, F. Mulargia, P. L. Rossi, "VS30: Proxy for seismic amplification?", Seismological Research Letters, Vol. 79, No. 4, pp. 540–543, 2008

[5] V. W. Lee, M. D. Trifunac, "Should average shear-wave velocity in the top 30m of soil be used to describe seismic amplification?", Soil Dynamics and Earthquake Engineering, Vol. 30, No. 11, pp. 1250–1258, 2010

[6] Building Seismic Safety Council, NEHRP recommended provisions for seismic regulations for new buildings and other structures, Part 1: Provisions (FEMA 368), Federal Emergency Management Agency, 2001

[7] AASHTO (American Association of State Highway and Transportation Officials), Guide specifications for LRFD seismic bridge design, Second edition with 2014 interim, AASHTO, 2014

[8] CEN, Eurocode8. Design of structures for earthquake resistance. Part1: general rules, seismic actions and rules for buildings. Final draft pr EN1998, European Committee for Standardization, CEN, 2003

[9] Building Seismic Safety Council, Recommended provisions for seismic regulations for new buildings and other structures, part 1: Provisions. report No. FEMA-450, FEMA, 2003

[10] American Society of Civil Engineers (ASCE), Minimum design loads for buildings and other structures, tandards ASCE/SEI 7-10, 2010

[11] J. X. Zhao, J. Zhang, A. Asano, Y. Ohno, T. Oouchi, T. Takahashi, H. Ogawa, K. Irikura, H. K. Thio, P. G. Somerville, Y. Fukushima, Y. Fukushima, "Attenuation relations of strong ground motion in Japan using site classification based on predominant period", Bulletin of the Seismological Society of America, Vol. 96, No. 3, pp. 898–913, 2006

[12] T. Kanno, A. Narita, N. Morikawa, H. Fujiwara, Y. Fukushima, "A new attenuation relation for strong ground motion in Japan based on recorded data", Bulletin of the Seismological Society of America, Vol. 96, No. 3, pp. 879–897, 2006

[13] Japan Road Association, Specifications for highway bridges, part5, Seismic design, ver. 2012, Maruzen Co., Ltd., 2016

[14] T. Narafu, Y. Ishiyama, R. Ison, J. Sakuma, H. Kato, S. Kita, "Outline and features of Japanese seismic design code", 16th World Conference on Earthquake Engineering, Santiago Chile, January 9-13, 2017

[15] D. M. Boore, W B. Joyner, "Site amplifications for generic rock sites", Bulletin of the Seismological Society of America, Vol. 87, No. 2, pp. 327-341, 1997

[16] Y. Fukushima, T. Nagao, "Variation of earthquake ground motions with focus on site amplification factors: a case study", Engineering, Technology & Applied Science Research Vol. 9, No. 4, pp. 4355-4360, 2019

[17] S. Aoi, K. Obara, S. Hori, K. Kasahara, Y. Okada, "New strong-motion observation network: KiK-net", Eos, Transactions of the American Geophysical Union, Vol. 81, 2000

[18] H. Fujiwara, S. Kawai, K. X. S. Hao, N. Morikawa, H. Azuma, "J-SHIS: An integrated system for sharing information on national seismic hazard maps for Japan", 16th World Conference on Earthquake Engineering, Santiago Chile, January 9-13, 2017

[19] Y. Okada, K. Kasahara, S. Hori, K. Obara, S. Sekiguchi, H. Fujiwara, A. Yamamoto, "Recent progress of seismic observation networks in Japan-Hi-net, F-net, K-NET and KiK-net", Earth Planets and Space, Vol. 56, No. 8, pp. 15-28, 2004